Aspergillus latus: a cryptic causative agent of aspergillosis emerging in Japan

Saho Shibata[1], Momotaka Uchida[1], Sayaka Ban[1], Katsuhiko Kamei[1], Akira Watanabe[1], Takashi Yaguchi[1], Vit Hubka[2,3], Hiroki Takahashi[1,4,5]

[1]Medical Mycology Research Center, Chiba University, 1-8-1 Inohana, Chuo-ku, Chiba 260-8673, Japan

[2]Laboratory of Fungal Genetics and Metabolism, Institute of Microbiology, Czech Academy of Sciences, Vídeňská 1083, 142 00 Prague 4, Czech Republic

[3]Department of Botany, Faculty of Science, Charles University, Benátská 2, 128 00 Prague 2, Czech Republic

[4]Molecular Chirality Research Center, Chiba University, 1-33 Yayoi-cho, Inage-ku, Chiba 263-8522, Japan.

[5]Plant Molecular Science Center, Chiba University, 1-8-1 Inohana, Chuo-ku, Chiba 260-8675, Japan.

Address for correspondence: Hiroki Takahashi

E-mail: hiroki.takahashi@chiba-u.jp

ORCID

S. Shibata: 0000-0003-2336-6948

M. Uchida: 0000-0001-5642-1435

S. Ban: 0000-0003-3442-308X

K. Kamei: 0000-0002-6067-9049

A. Watanabe: 0000-0002-3057-2937

T. Yaguchi: 0000-0002-9697-8470

V. Hubka: 0000-0003-4583-6496

H. Takahashi: 0000-0001-5627-1035

Abstract

Allodiploid hybrid species, *Aspergillus latus*, belonging to section *Nidulantes*, is a hybrid of *A. spinulosporus* and unknown species closely related to *A. quadrilineatus* and *A. subltus*. This hybrid has often been misidentified as the species in section *Nidulantes*, such as *A. nidulans*, *A. spinulosporus*, *A. sublatus*, or other cryptic species. *A. latus* has not been reported in Japan as well as Asia so far. In this study, we screened 23 clinical strains identified as *A. spinulosporus* isolated in Japan from 2012 to 2023 and found seven *A. latus* strains. To characterize the *A. latus* strains, we conducted comprehensive phenotyping including morphological observation, whole genome sequences and phylogenetic analysis based on calmodulin (*CaM*) gene. In addition, we conducted antifungal susceptibility testing for *A. latus* strains. As a result, the morphological characters of *A. latus* were more similar to those of *A. spinulosporus* compared to *A. sublatus*. However, the ascospore of *A. latus* differed from that of *A. spinulosporus*. *A. latus* phylogenetically clustered with *A. spinulosporus* and *A. sublatus*. Furthermore, *A. latus* strains showed reduced susceptibility to caspofungin and amphotericin B compared to *A. spinulosporus*, while they were susceptible to azoles. Our results suggest that *A. latus* has been a causative pathogen of aspergillosis in Japan since 2013.

Keywords: *Aspergillus latus*, *Aspergillus spinulosporus*, *Aspergillus sublatus*, section *Nidulantes*, aspergillosis

Introduction

Aspergillus species are the causal agents for aspergillosis, mainly affecting immunocompromised individuals [1, 2]. Although *A. fumigatus* is a main causative agent, other species such as *A. nidulans*, *A. flavus*, *A. niger*, and *A. terreus* also contribute to the disease [3–6]. *Aspergillus nidulans*, a member of the section *Nidulantes* poses a serious threat to immunocompromised patients, especially those with chronic granulomatous disease [3]. Additionally, eleven other species within the section *Nidulantes* have been isolated from patients with invasive aspergillosis [7]. Recently, Steenwyk et al. (2020) through screening of *A. nidulans* strains identified that *A. latus* is an allodiploid hybrid species between *A. spinulosporus* and unknown species closely related to *A. quadrilineatus*, and exhibits higher virulence and minimum inhibitory concentrations to some antifungals than *A. nidulans* [8]. This highlights the importance of accurate species identification to ensure effective treatment, as misidentification could compromise patient care.

Steenwyk et al. (2020 & 2024) reported 30 *A. latus* strains from Belgium, Brazil, France, Germany, Netherlands and Portugal identified as *A. nidulans*, *A. spinulosporus*, or other cryptic species, suggesting that *A. latus* infections are likely underreported [9]. Prospective survey in single center in Japan reported that six *A. nidulans* strains were identified among 107 *Aspergillus* strains [11]. To date, *A. latus* has not been reported in Asia including Japan.

However, *A. nidulans* and some cryptic species were isolated from patients in Japan, namely *A. latus* could had also been isolated [10, 11].

In this study, we identified seven clinical *A. latus* strains isolated in Japan by screening 23 *A. spinulosporus* strains which were collected between 2012 and 2023. To characterize these seven *A. latus* strains isolated in Japan, we performed comprehensive phenotyping including morphological observations, whole genome sequences and phylogenetic analysis based on calmodulin (*CaM*) gene. In addition, we measured the antifungal susceptibility of these strains to six antifungals. Here, we present the first report of *A. latus* being isolated in Japan. Our findings indicate that *A. latus* has been the causative agent of aspergillosis in Japan since 2013.

Material and methods

Strains

A. latus, *A. sublatus* and *A. spinulosporus* strains used in this study have been stored and maintained at the Medical Mycology Research Center, Chiba University (IFM strains) in Japan. A total of 23 strains of *A. latus* and *A. spinulosporus* are clinical isolate in Japan, and *A. sublatus* IFM 42029 (= IFM 4553 = CBS 140630) is a type strain collected from soil in Brazil.

Genomic DNA extraction

Fungi were incubated on Potato Dextrose Agar (Thermo Fischer Scientific, MA, USA) at 30 °C for 7 days to obtain fully mature conidia. The conidia were inoculated in Potato Dextrose Broth (Thermo Fischer Scientific) at 37 °C at 180 rpm for 16 h. Mycelia were washed with H_2O, and genomic DNA was purified with phenol-chloroform extraction and Monarch® Genomic DNA Purification Kit (New England Biolabs, MA, USA) [12, 13]. The DNA concentration and quality were then measured by Qubit Fluorometer (Thermo Fischer Scientific). The extracted DNA were used for cloning of *CaM* gene and whole-genome sequencing.

Whole genome sequencing and assembly

Whole-genome 150 bp paired-end (PE) sequencing of four *A. latus* strains, IFM 65030, IFM 65233, IFM 65239 and IFM 66778 was performed using Illumina NovaSeq 6000 (Illumina, CA, USA) by Novogene Biotech Co. (Beijing, China). The raw genomic reads were trimmed using fastp v.0.20.1 [14]. The mitochondrial genomes were assembled using GetOrganelle v.1.6.4 [15]. To filter the mitochondrial reads, the reads were aligned with the mitochondrial genome using BWA-MEM v.0.7.17-r1188 [16]. The mapped reads were filtered using SAMtools v.1.10 [17] and SeqKit v.0.10.1 [18]. The nuclear genomes were assembled using VelvetOptimiser v.2.2.6 [19].

The completeness of draft genomes was evaluated by BUSCO v. 5.2.1 [20] with the database eurotiales_odb10. blastn v.2.15.0+ [21] was used for extracting the sequences of *CaM* of *A. latus* strains by serving the sequence of *A. nidulans* FGSC A4 as query sequence. The genome sizes of *A. latus* strains were estimated using Jellyfish [22] and GenomeScope with 21 k-mers [23].

DNA Cloning and Sequencing

The cloning of two *CaM* genes of three strains, IFM 61956, IFM 63852 and IFM 64630, were performed. PCR amplification was performed by Quick Taq® HS DyeMix (TOYOBO, Tokyo, Japan) in a ProFlex™ PCR System (Thermo Fisher Scientific) with a program consisting of an initial denaturing step at 94 °C for 2 min: 35 cycles of denaturation at 94 °C for 30 sec, annealing at 50 °C for 30 sec, and extension at 68 °C for 1 min. The amplicons of *CaM* were obtained by PCR with primer pairs CF1L_SacI (5′-AAAGAGCTCGCCGACTCTTTGACYGARGAR-3′) and CF4_SacI (5′-AAAGAGCTCTTTYTGCATCATRAGYTGGAC-3′). These primers contain the sequence of CF1 and CF4 primers, respectively, from a previous study [24, 25], with the SacI restriction site at the 5′ end. The PCR amplicons were purified by gel extraction with QIAquick Gel Extraction Kit (QIAGEN, Hilden, Germany). The objective gene fragments were cloned into

pMK-dGFP vector [26], and introduced into competent cells of *Escherichia coli* DH5α. FastGene Plasmid Mini Kit (Nippon Genetics, Tokyo, Japan) was used to extract the plasmid DNA. The plasmid (ca. 2.0 µL) was used as the templates for the sequencing reaction with a BigDye Terminator v3.1 Cycle Sequencing Kit (Thermo Fisher Scientific) along with PtrpC-Rev (5′-AAATGCTCCTTCAATATCATCTTCTGTCGA-3′) and M13R (5′-CAGGAAACAGCTATGAC-3′) primers [27], following the manufacturer's instructions. Ethanol precipitation was used to remove excess fluorescent dye-terminators from cycle sequencing reactions prior to analysis on an automated sequencer. Sequence was performed with an ABI 3100 Genetic Analyzer (Thermo Fisher Scientific).

Phylogenetic analysis

The sequences of *CaM* ranging from 438 bp to 824 bp in length were aligned with MAFFT v.7.508 [28, 29]. Aligned sequences were trimmed using trimAl v.1.4.rev15 [30], resulting in 686 bp in length. The maximum likelihood tree of *CaM* was constructed using the multithreaded version of RAxML v.8.2.12 [31], the GTRCAT model, and 1,000 bootstrap replicates. The phylogenetic tree was visualized using the FigTree (free download available at http://tree.bio.ed.ac.uk/software/figtree/). A total of 112 taxa were included in our tree (Supplementary Table S1).

Morphological observations

A. latus IFM 65329 was used for microscopic and macroscopic observation. The colony character of the other six strains of *A. latus*, *A. sublatus* IFM 42029^{T} (= IFM 4553^{T}) and *A. spinulosporus* IFM 66771 were observed. The observations of macroscopic characters were curried on the agar media, i.e., Czapek yeast autolysate agar (CYA, Czapeck Dox Agar, Duchefa Biochemie, Haarlem, Netherlands and Difco™ Yeast Extract, Thermo Fischer Scientific), oatmeal agar (OA, Sigma Aldrich, MO, USA) and malt extract agar (MEA, Thermo Fischer Scientific) with trace elements (0.1 g $ZnSO_4 \cdot 7H_2O$ and 0.5 g $CuSO_4 \cdot 5H_2O$ in 100 mL distilled water) at 25 or 37 °C for 7 days. Microscopic observations of conidia and conidiophores were made from 1 week old colonies on MEA. Ascomata and ascospores were observed from 8-week-old colonies on OA. A light microscope (Nikon ECLIPSE Ni, Tokyo, Japan and Swift Optical Instruments S7-TP520, TX, USA) was used to examine morphological characters including the size and shape of ascomata, ascospores, conidiophores and conidia. These were mounted in a drop of water on glass slides. The slide preparations were examined and photographed using a digital camera (Nikon DS-Fi3, Japan). Approximately 30 structures were randomly chosen, and their length and width were measured using 'ImageJ' software (free download available at http://rsbweb.nih.gov/ij/).

Antifungal susceptibility testing

Minimum inhibitory concentration (MIC) tests for amphotericin B (AMPH-B), itraconazole (ITCZ), voriconazole (VRCZ), miconazole (MCZ), micafungin (MCFG), and caspofungin (CPFG), were performed using the dried plate for antifungal susceptibility testing of yeasts method (Eiken Chemicals, Tokyo, Japan). The method follows the Clinical and Laboratory Standards Institute M38-E2 with slight modifications [32–34].

Results

Screening and identification of *A. latus*

To identify the presence of allodiploid hybrid strains of *A. latus*, we sequenced the *CaM* genes of 23 *A. spinulosporus* strains. Sequences with double peaks were observed in seven strains. The sequences of two copies of *CaM* were determined in all seven strains by either cloning or whole-genome sequencing (Table 1). These strains were isolated from the patients between 2013 and 2022. The ages of the patients ranged from 13 to 79 years. The patients were diagnosed with invasive pulmonary aspergillosis (IFM 63852 and IFM 66778) and chronic pulmonary aspergillosis (IFM 65233 and IFM 65329), the other patients were not diagnosed with aspergillosis (IFM 61956, IFM 64360, and IFM 65030). However, the patients were

diagnosed with other diseases such as leukemia. Therefore, we could not conclude that *A. latus* is a primary cause of death.

Draft genomes for four *A. latus* strains (IFM 65030, IFM 65233, IFM 65239 and IFM 66778) were generated, with assembled genome sizes ranging from 62.1 Mb to 63.2 Mb, aligning with the typical genome sizes of *A. latus* (previous study showed average genome size 69.09 ± 5.68 Mb [8]) (Supplementary Table S2).

Phylogenetic analysis

We conducted a phylogenetic analysis to characterize the position of seven Japanese *A. latus* strains. One copy of *CaM* gene sequence clustered with the sequences of *A. spinulosporus*, while the other copy clustered with *A. sublatus* (Fig. 1). The *CaM* sequence of *A. latus* differed from that of *A. sublatus* in length by 1 bp, that of *A. quadrilineatus* in length by 6 bp, but the *CaM* sequence of *A. latus* harbors no specific substitution compared to *A. sublatus*, *A. quadrilineatus* and *A. spinulosporus.*

Morphological observations

The colony morphologies of *A. latus* varied among strains (Fig. 2, Supplementary Fig. 1). On MEA, the growth was slower compared to that of *A. sublatus* and *A. spinulosporus* (Fig. 2B,

Supplementary Fig. 1B, E, H, K, N, Q, T, W). In terms of colony appearance, *A. latus* was more similar to *A. spinulosporus* than to *A. sublatus*, as its colonies were covered with green conidia on OA and sometimes on CYA (Table 2 and Supplementary Fig. 1C, F, I, L, O, R, X). The microscopic of *A. latus* also closely resembled those of the other two species but ascospores of *A. spinulosporus* are echinulated (Table 2) [35, 36].

Antifungal susceptibility testing

Antifungal susceptibility testing was conducted on seven *A. latus*, one *A. sublatus*, and three *A. spinulosporus* strains (Table 3). Reduced susceptibility to CPFG was observed in all tested strains, geometric mean MICs of 7.2 for *A. latus*, 16 for *A. sublatus*, and 5.0 for *A. spinulosporus*. Reduced susceptibility to AMPH-B was noted in *A. latus* and *A. sublatus*, while *A. spinulosporus* strains displayed low MICs, with geometric mean MICs of 4.4, 4.0, and 0.7, respectively. *Aspergillus latus* strains displayed low MICs to MCFG, whereas MICs of *A. sublatus*, and *A. spinulosporus* were elevated. Susceptibility to VRCZ and MCZ varied: reduced susceptibility to VRCZ was observed in *A. latus* IFM 66778 strain (MIC 2.0), and reduced susceptibility to MCZ was noted in *A. latus* strains IFM 61956 and IFM 65329 (MIC 2.0), as well as *A. sublatus*. All tested strains were susceptible to ITCZ.

Discussion

Here, we report the allodiploid hybrid *A. latus* strains isolated in Japan. Although 30 strains have been found worldwide [8, 9], *A. latus* has not been reported in Japan as well as Asia. By screening 23 *A. spinulosporus* strains, we found seven clinical *A. latus* strains (30.4%). *A. latus* IFM 61956 was isolated in 2013, suggesting that this species might be more prevalent in the country. The pathogenicity of *A. latus* was shown to be comparable to that of *A. spinulosporus* and *A. nidulans* [8, 9]. In this study, the pathogenicity of *A. latus* was unclear, because *A. latus* strains could be colonized in most cases (Table 1). However, ongoing monitoring is necessary, as changes in pathogenicity or resistance profiles could impact treatment strategies in the future.

We conducted a phylogenetic analysis of *A. latus* (Fig. 1) with results indicating that it is derived from a hybridization between *A. spinulosporus* and a species related to *A. sublatus* and *A. quadrilineatus*. Morphological characters of seven *A. latus* strains, such as colony color and growth on MEA, were most stable among strains (Fig. 2B, Table 2, and Supplementary Fig. 1B, E, H, K, N, Q). The differences between *A. latus*, *A. spinulosporus* and *A. sublatus*, however, were slight, and given the variability observed in previous studies, species identification relying on these traits may be challenging (Supplementary Fig. 1) [9].

In terms of antifungal susceptibility, strains of *A. latus* found in Japan demonstrated increased susceptibility to ITCZ compared to overseas strains [8], while showing reduced

susceptibility to CPFG, aligning with the previous research [8, 9] (Table 3). It has been reported that *A. spinulosporus* exhibits reduced susceptibility to CPFG compared to *A. nidulans* and other clinically relevant species in section *Nidulantes* [8, 37]. In this study, we confirmed that *A. spinulosporus* and *A. sublatus* showed reduced susceptibility to CPFG, suggesting that this characteristic in *A. latus* may be derived from these species. In addition, *A. latus* strains exhibited AMPH-B resistance. Although high AMPH-B MIC values have been reported in other *Aspergillus* species, especially *A. nidulans* and related species [8, 37, 38], the mechanisms underlying the resistance remain poorly understood. Increased catalase production has been implicated in AMPH-B resistance in *A. terreus* [39], suggesting that *A. latus* may produce high level of catalase.

In conclusion, our study provides significant insights into the ecology and clinical relevance of *A. latus*, a newly recognized hybrid pathogen and cryptic species of *A. nidulans*. We documented the first occurrence of this pathogen in Japan, demonstrating its prevalence and potential role as a causative agent of aspergillosis since 2013. The comprehensive phenotyping, including morphological and genetic analysis, underscored the diagnostic challenges due to its similarities with *A. spinulosporus* and *A. sublatus*. Moreover, antifungal susceptibility testing revealed reduced susceptibility to certain antifungal agents, highlighting the need for accurate identification to inform effective treatment strategies. Our findings add to the growing body of

knowledge about the distribution and pathogenic characteristics of *A. latus* and emphasize the importance of continued surveillance and accurate diagnostics in clinical mycology.

Acknowledgements

We thank Dr Takayuki Arazoe (Tokyo University of Science) for providing us with the pMK-dGFP plasmid. We thank Junko Ito and Emi Shirai for technical assistance with the experiments. We are also grateful to Machiko Zen for assistance with the data analysis.

References

1. Latgé JP. *Aspergillus fumigatus* and aspergillosis. Clin Microbiol Rev. 1999;12:310–50. https://doi.org/10.1128/CMR.12.2.310
2. Sugui JA, Kwon-Chung KJ, Juvvadi PR, Latgé J-P, Steinbach WJ. *Aspergillus fumigatus* and related species. Cold Spring Harb Perspect Med. 2014;5:a019786. https://doi.org/10.1101/cshperspect.a019786
3. Bastos RW, Valero C, Silva LP, Schoen T, Drott M, Brauer V, et al. Functional Characterization of Clinical Isolates of the Opportunistic Fungal Pathogen *Aspergillus nidulans*. mSphere. 2020;5:e00153-20. https://doi.org/10.1128/mSphere.00153-20

4. Paulussen C, Hallsworth JE, Álvarez-Pérez S, Nierman WC, Hamill PG, Blain D, et al. Ecology of aspergillosis: insights into the pathogenic potency of *Aspergillus fumigatus* and some other *Aspergillus* species. Microb Biotechnol. 2017;10:296–322. https://doi.org/10.1111/1751-7915.12367

5. Zakaria A, Osman M, Dabboussi F, Rafei R, Mallat H, Papon N, et al. Recent trends in the epidemiology, diagnosis, treatment, and mechanisms of resistance in clinical *Aspergillus* species: A general review with a special focus on the Middle Eastern and North African region. J Infect Public Health. 2020;13:1–10. https://doi.org/10.1016/j.jiph.2019.08.007

6. Hashimoto A, Hagiwara D, Watanabe A, Yahiro M, Yikelamu A, Yaguchi T, et al. Drug Sensitivity and Resistance Mechanism in *Aspergillus* Section *Nigri* Strains from Japan. Antimicrob Agents Chemother. 2017;61:e02583-16. https://doi.org/10.1128/AAC.02583-16

7. Arastehfar A, Carvalho A, Houbraken J, Lombardi L, Garcia-Rubio R, Jenks JD, et al. *Aspergillus fumigatus* and aspergillosis: From basics to clinics. Stud Mycol. 2021;100:100115. https://doi.org/10.1016/j.simyco.2021.100115

8. Steenwyk JL, Lind AL, Ries LNA, Dos Reis TF, Silva LP, Almeida F, et al. Pathogenic Allodiploid Hybrids of *Aspergillus* Fungi. Curr Biol. 2020;30:2495-2507.e7. https://doi.org/10.1016/j.cub.2020.04.071

9. Steenwyk JL, Knowles S, Bastos RW, Balamurugan C, Rinker D, Mead ME, et al. Evolutionary origin and population diversity of a cryptic hybrid pathogen. Nat Commun. 2024;15:8412. https://doi.org/10.1038/s41467-024-52639-1

10. Tashiro T. Pulmonary Aspergillosis and clinical significance of *Aspergillus* isolation from respiratory samples. J Jap Soc Clin Microbiol. 2009;19:67–75.

11. Toyotome T, Saito S, Koshizaki Y, Komatsu R, Matsuzawa T, Yaguchi T. Prospective survey of *Aspergillus* species isolated from clinical specimens and their antifungal susceptibility: A five-year single-center study in Japan. J Infect Chemother. 2020;26:321–3. https://doi.org/10.1016/j.jiac.2019.09.002

12. Bian C, Kusuya Y, Sklenář F, D'hooge E, Yaguchi T, Ban S, et al. Reducing the number of accepted species in *Aspergillus* series *Nigri*. Stud Mycol. 2022;102:95–132. https://doi.org/10.3114/sim.2022.102.03

13. Kusuya Y, Bian C, Hagiwara D, Ban S, Takahashi H. A novel Zn2-Cys6 transcription factor clcA contributes to copper homeostasis in *Aspergillus fumigatus*. Curr Genet. 2022;68:605–17. https://doi.org/10.1007/s00294-022-01250-2

14. Chen S, Zhou Y, Chen Y, Gu J. fastp: an ultra-fast all-in-one FASTQ preprocessor. Bioinformatics. 2018;34:i884–90. https://doi.org/10.1093/bioinformatics/bty560

15. Jin J-J, Yu W-B, Yang J-B, Song Y, dePamphilis CW, Yi T-S, et al. GetOrganelle: a fast and versatile toolkit for accurate de novo assembly of organelle genomes. Genome Biol. 2020;21:241. https://doi.org/10.1186/s13059-020-02154-5

16. Li H, Durbin R. Fast and accurate short read alignment with Burrows-Wheeler transform. Bioinformatics. 2009;25:1754–60. https://doi.org/10.1093/bioinformatics/btp324

17. Danecek P, Bonfield JK, Liddle J, Marshall J, Ohan V, Pollard MO, et al. Twelve years of SAMtools and BCFtools. Gigascience. 2021;10:giab008. https://doi.org/10.1093/gigascience/giab008

18. Shen W, Le S, Li Y, Hu F. SeqKit: A Cross-Platform and Ultrafast Toolkit for FASTA/Q File Manipulation. PLoS One. 2016;11:e0163962. https://doi.org/10.1371/journal.pone.0163962

19. Zerbino DR, Birney E. Velvet: algorithms for de novo short read assembly using de Bruijn graphs. Genome Res. 2008;18:821–9. https://doi.org/10.1101/gr.074492.107

20. Seppey M, Manni M, Zdobnov EM. BUSCO: Assessing Genome Assembly and Annotation Completeness. Methods Mol Biol. 2019;1962:227–45. https://doi.org/10.1007/978-1-4939-9173-0_14

21. Camacho C, Coulouris G, Avagyan V, Ma N, Papadopoulos J, Bealer K, et al. BLAST+: architecture and applications. BMC Bioinformatics. 2009;10:421. https://doi.org/10.1186/1471-2105-10-421

22. Marçais G, Kingsford C. A fast, lock-free approach for efficient parallel counting of occurrences of k-mers. Bioinformatics. 2011;27:764–70. https://doi.org/10.1093/bioinformatics/btr011

23. Vurture GW, Sedlazeck FJ, Nattestad M, Underwood CJ, Fang H, Gurtowski J, et al. GenomeScope: fast reference-free genome profiling from short reads. Bioinformatics. 2017;33:2202–4. https://doi.org/10.1093/bioinformatics/btx153

24. Peterson SW. Multilocus DNA sequence analysis shows that *Penicillium biourgeianum* is a distinct species closely related to *P. brevicompactum* and *P. olsonii*. Mycol Res. 2004;108:434–40. https://doi.org/10.1017/S0953756204009761

25. Peterson SW, Vega FE, Posada F, Nagai C. *Penicillium coffeae*, a new endophytic species isolated from a coffee plant and its phylogenetic relationship to *P. fellutanum*, *P. thiersii* and *P. brocae* based on parsimony analysis of multilocus DNA sequences. Mycologia. 2005;97:659-66. https://doi.org/10.3852/mycologia.97.3.659

26. Arazoe T, Ohsato S, Arie T, Yoneyama K, Kuwata S. Construction of a system for exploring mitotic homologous recombination in the genome of *Pyricularia oryzae*. J Gen Plant Pathol. 2013;79:422–30. https://doi.org/10.1007/s10327-013-0474-2

27. Huey B, Hall J. Hypervariable DNA fingerprinting in *Escherichia coli*: minisatellite probe from bacteriophage M13. J Bacteriol. 1989;171:2528–32. https://doi.org/10.1128/jb.171.5.2528-2532.1989

28. Katoh K, Misawa K, Kuma K, Miyata T. MAFFT: a novel method for rapid multiple sequence alignment based on fast Fourier transform. Nucleic Acids Res. 2002;30:3059–66. https://doi.org/10.1093/nar/gkf436

29. Katoh K, Standley DM. MAFFT multiple sequence alignment software version 7: improvements in performance and usability. Mol Biol Evol. 2013;30:772–80. https://doi.org/10.1093/molbev/mst010

30. Capella-Gutiérrez S, Silla-Martínez JM, Gabaldón T. trimAl: a tool for automated alignment trimming in large-scale phylogenetic analyses. Bioinformatics. 2009;25:1972–3. https://doi.org/10.1093/bioinformatics/btp348

31. Stamatakis A. RAxML version 8: a tool for phylogenetic analysis and post-analysis of large phylogenies. Bioinformatics. 2014;30:1312–3. https://doi.org/10.1093/bioinformatics/btu033

32. Kikuchi K, Watanabe A, Ito J, Oku Y, Wuren T, Taguchi H, et al. Antifungal susceptibility of *Aspergillus fumigatus* clinical isolates collected from various areas in Japan. J Infect Chemother. 2014;20:336–8. https://doi.org/10.1016/j.jiac.2014.01.003

33. CLSI. Reference method for broth dilution antifungal susceptibility testing of filamentous fungi. In: CLSI standard M38, 3rd edn. Clinical and Laboratory Standards Institute, Wayne, PA; 2017.

34. He X, Kusuya Y, Hagiwara D, Toyotome T, Arai T, Bian C, et al. Genomic diversity of the pathogenic fungus *Aspergillus fumigatus* in Japan reveals the complex genomic basis of azole resistance. Commun Biol. 2024;7:274. https://doi.org/10.1038/s42003-024-05902-6

35. Chen AJ, Frisvad JC, Sun BD, Varga J, Kocsubé S, Dijksterhuis J, et al. *Aspergillus* section *Nidulantes* (formerly *Emericella*): Polyphasic taxonomy, chemistry and biology. Stud Mycol. 2016;84:1–118. https://doi.org/10.1016/j.simyco.2016.10.001

36. Horie Y. New or interesting *Emericella* from herbal drugs. Trans Mycol Soc Japan. 1979;20:481–91.

37. Tavakoli M, Rivero-Menendez O, Abastabar M, Hedayati MT, Sabino R, Siopi M, et al. Genetic diversity and antifungal susceptibility patterns of *Aspergillus nidulans* complex obtained from clinical and environmental sources. Mycoses. 2020;63:78–88. https://doi.org/10.1111/myc.13019

38. Van Der Linden JWM, Warris A, Verweij PE. *Aspergillus* species intrinsically resistant to antifungal agents. Med Mycol. 2011;49 Suppl 1:S82-89. https://doi.org/10.3109/13693786.2010.499916

39. Blum G, Perkhofer S, Haas H, Schrettl M, Würzner R, Dierich MP, et al. Potential basis for amphotericin B resistance in *Aspergillus terreus*. Antimicrob Agents Chemother. 2008;52:1553–5. https://doi.org/10.1128/AAC.01280-07

Statements & Declarations

Funding

This work was partly supported by JSPS KAKENHI Grant No. 24K19262.

Competing Interests

The authors have no relevant financial or non-financial interests to disclose.

Author Contributions

Saho Shibata, Vit Hubka, and Hiroki Takahashi contributed to the study conception and design. Material preparation, data collection and analysis were performed by Saho Shibata, Momotaka Uchida, Sayaka Ban, Kamei Katsuhiko, Akira Watanabe, Vit Hubka, and Hiroki Takahashi. The

draft of the manuscript was written by Saho Shibata, Momotaka Uchida, Takashi Yaguchi, Vit Hubka and Hiroki Takahashi, and all authors commented on the manuscript. All authors read and approved the final manuscript.

Ethical approval

No ethical approval is required

Table 1. Clinical information of *Aspergillus latus* strains examined in this study

Strain No.	Species name		Isolation year	Disease record	Age	Outcome
	this study	previous identified				
IFM 61956	*A. latus*	*A. spinulosporus*	2013	colon cancer, pneumonia	N/A	dead
IFM 63852	*A. latus*	*A. spinulosporus*	2016	interstitial lung disease, invasive pulmonary aspergillosis	79	dead
IFM 64360	*A. latus*	*A. spinulosporus*	2016	ulcerative colitis, pneumonia	45	dead
IFM 65030	*A. latus*	*A. spinulosporus*	2017	bronchiolitis	62	alive
IFM 65233	*A. latus*	*A. spinulosporus*	2018	liver cirrhosis, chronic pulmonary aspergillosis	66	alive
IFM 65329	*A. latus*	*A. spinulosporus*	2015	pulmonary non-tuberculous mycobacteriosis, chronic pulmonary aspergillosis	68	alive
IFM 66778	*A. latus*	*A. spinulosporus*	2020	acute myeloid leukemia, invasive pulmonary aspergillosis	13	alive

Table 2. Morphological comparison of *Aspergillus latus*, *A. spinulosporus* and *A. sublatus*.

		A. latus This study	*A. spinulosporus* This study & [35]	*A. sublatus* This study & [36]
Colony	CYA	Obverse: yellow green, olive green, pale brown edge	Obverse: pale brown, yellow edge, grey, green conidia forming all over	Obverse: reddish brown, grey, pale brown edge, reddish conidia forming in the center
		Reverse: dark brown, yellowish brown, green conidia formed in the center	Reverse: pale brow, brown,	Reverse: pale brown, orange, brown edge
	MEA	Obverse: pale yellow, irregular edge with white mycelia	Obverse: concentrically growth, pale-yellow	Obverse: concentrically growth, pale-yellow, white edge, olive-green conidia formed in the center
		Reverse: pale-yellow, soluble yellowish pigments present and exudates absent	Reverse: pale yellow, soluble pigments and exudates absent	Reverse: pale yellow, no soluble pigments and exudates
	OA	Obverse: pale brown, green, partially reddish, covered in green conidia, the center pigmented yellow to brown	Obverse: pale brown with olive green conidia and sometime wrinkled	Obverse: brown with pale brown edge
		Reverse: soluble orange or brown pigments present and exudates absent	Reverse: orange to brown, brown soluble pigments present and exudates absent	Reverse: orange to brown, brown soluble pigments present and exudates absent
Ascoma	character	cleistothecial, superficial, black, globose, subglobose, surrounded by Hülle cells	cleistothecial, superficial, dark brown, globose, subglobose, surrounded by Hülle cells	cleistothecial, superficial, red to purple, globose, subglobose

Hülle cells	size (μm)	8.7–20 (diameter)	14–30 (diameter)	12.5–30× 10–28
	character	hyaline, globose to ovoid	hyaline, globose to ovoid	hyaline, globose to ovoid
Ascospores	size (μm)	3.5–10 (pleated equatorial crests: 0.6–2.3)	3.5–4.5 × 3.0–4.5 (pleated equatorial crests: 0.8–1.0)	4.0–4.5 × 3.0–3.5 (pleated equatorial crests: 1.0–1.5)
	character	purple red, reddish brown, in surface view globose, subglobose, spore bodies smooth, incompletely reticulate, ribbed, globose, subglobose, in side view lenticular, with two pleated equatorial crests	orange,reddish brown, in surface view globose, subglobose, spore bodies echinulate, globose, subglobose, in side view lenticular	purple red, reddish brown, globose, subglobose, spore bodies smooth, in side view lenticular
Conidiophores	size (μm)	50–179 × 2.0–3.6	70–120 × 5.0–6.0	200× 4.0–6.0
	character	smooth stipes, pale brown	smooth stipes, yellowish brown	pale grey, grayish yellow
Vesicles	size (μm)	4.8–9.0 (wide)	9.0–11 (wide)	9.0–12.5 (wide)
	character	pale brown, subglobose to subclavate	yellowish brown, subclavate, fertile over the upper half	hemispherical, flask-shaped
Metulae	size (μm)	5.1–8.3 × 2.0–4.0	6.0–8.0 × 3.0–4.0	4.0–6.0 × 3.0–4.0
	character	hyaline to pale green	pale brown to pale green	hyaline to pale yellowish brown
Phialides	size (μm)	5.2–8.4 × 2.0–4.0	6.0–8.5 × 2.0–3.0	6.0–8.0 × 2.0–3.0
	character	hyaline, flask-shaped	hyaline to pale green, flask-shaped	hyaline to pale yellowish brown
Conidia	size (μm)	2.7–4.8	3.0–4.0	2.5–3.5(4.0)
	character	echinulate, globose to subglobose, green in mass	echinulate, globose to subglobose, green in mass	echinulate, globose to subglobose, green to pale olive green

394

Table 3. MIC values for antifungal drugs

Species name	Strain No.	MIC (μg/mL)					
		MCFG	CPFG	AMPH-B	ITCZ	VRCZ	MCZ
Aspergillus latus	IFM 61956	0.06	16	4	0.5	0.12	2
	IFM 63852	0.12	16	4	0.25	0.12	1
	IFM 64360	0.06	16	4	0.25	0.25	1
	IFM 65030	0.06	4	4	0.25	0.06	1
	IFM 65233	0.06	2	4	0.5	0.06	1
	IFM 65329	0.03	8	4	0.25	0.12	2
	IFM 66778	0.06	4	8	0.25	2	0.5
A. sublatus	IFM 42029^{T}	>16	16	4	0.25	0.12	2
A. spinulosporus	IFM 66771	0.15>	2	1	0.25	0.25	0.5
	IFM 61449	>16	8	0.5	0.25	0.12	0.5
	IFM 64750	>16	8	1	0.25	0.12	1

MCFG = micafungin, CPFG = caspofungin, AMPH-B = amphotericin B, ITCZ = itraconazole, VRCZ = voriconazole, MCZ = miconazole

Figure legends

Fig. 1. Phylogenetic tree constructed using maximum likelihood (ML) analysis based on the models selected with the GTRCAT for *CaM* (Bootstrap value: > 70%). *A. aurantiobrunneus* and *A. fructus* were used as outgroup. Numbers after taxa are isolate, specimen or strain numbers. The scale bar represents the number of nucleotide substitutions per site. The sequences obtained in this study are shown in bold. T = type sequence.

Fig. 2. *A. latus* IFM 65329 colonies: obverse CYA 37 °C (A), MEA 37 °C (B), OA 25 °C (C), reverse: CYA 37 °C (D), MEA 37 °C (E), OA 25 °C, 7d (F), conidiophores (G–J), conidia (K), Hülle cells (L), ascomata (M), ascospores (N, O) Scale bars: G–L, N, O 10 μm.

Shibata et al.
Figure 1

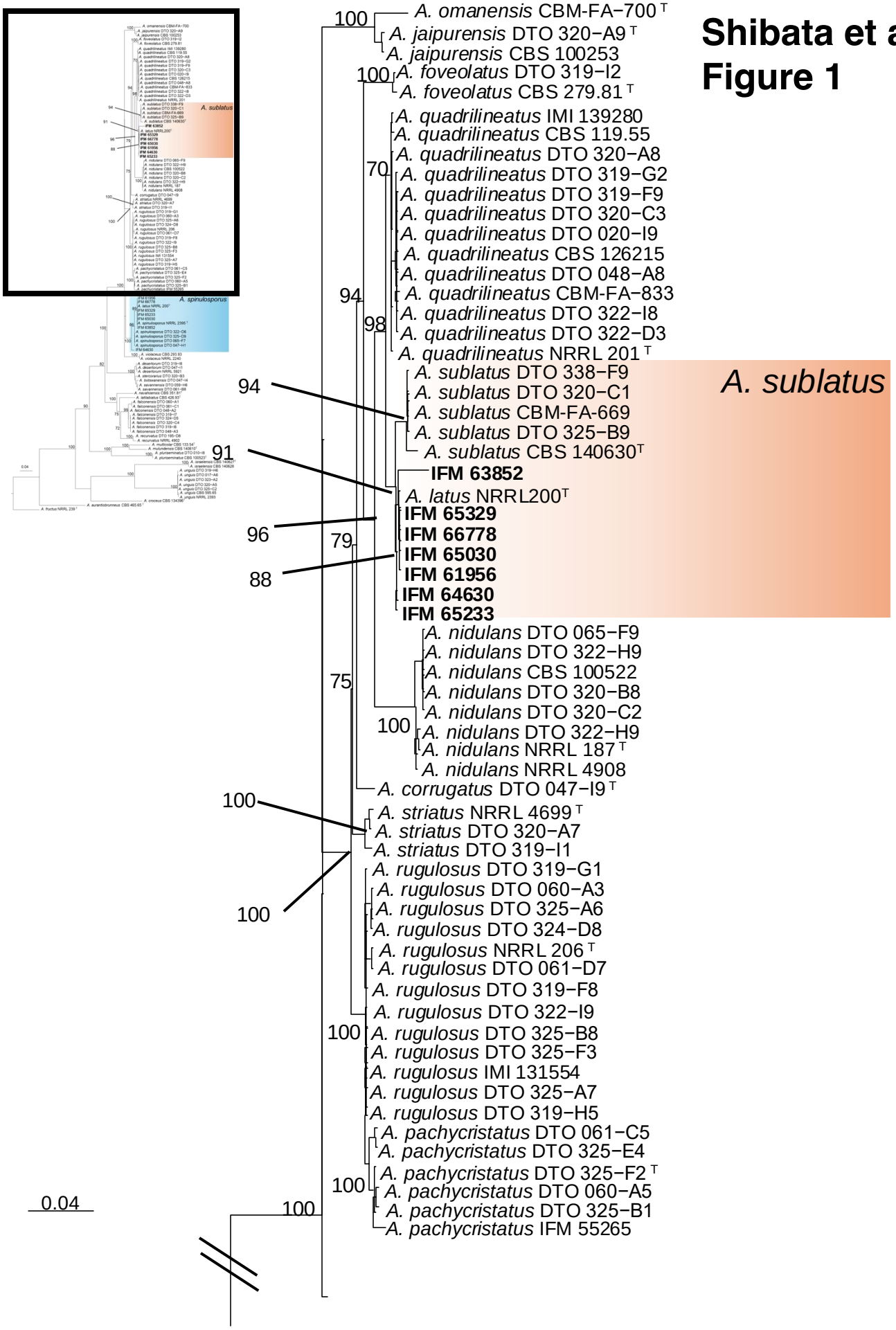

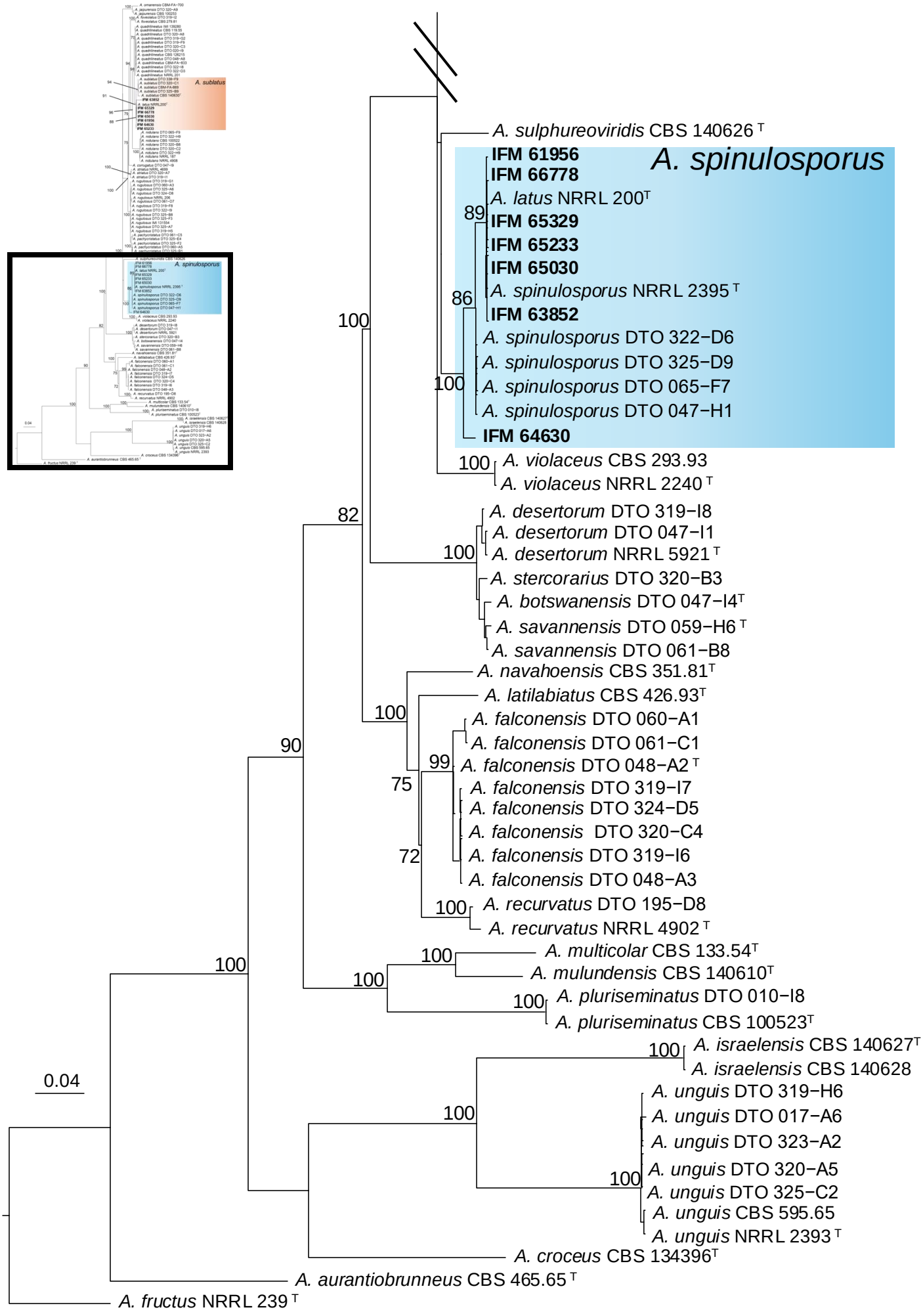
A. sublatus
A. spinulosporus
A. sulphureoviridis CBS 140626 T
IFM 61956
IFM 66778
A. latus NRRL 200T
IFM 65329
IFM 65233
IFM 65030
A. spinulosporus NRRL 2395 T
IFM 63852
A. spinulosporus DTO 322−D6
A. spinulosporus DTO 325−D9
A. spinulosporus DTO 065−F7
A. spinulosporus DTO 047−H1
IFM 64630
A. violaceus CBS 293.93
A. violaceus NRRL 2240 T
A. desertorum DTO 319−I8
A. desertorum DTO 047−I1
A. desertorum NRRL 5921 T
A. stercorarius DTO 320−B3
A. botswanensis DTO 047−I4T
A. savannensis DTO 059−H6 T
A. savannensis DTO 061−B8
A. navahoensis CBS 351.81T
A. latilabiatus CBS 426.93T
A. falconensis DTO 060−A1
A. falconensis DTO 061−C1
A. falconensis DTO 048−A2 T
A. falconensis DTO 319−I7
A. falconensis DTO 324−D5
A. falconensis DTO 320−C4
A. falconensis DTO 319−I6
A. falconensis DTO 048−A3
A. recurvatus DTO 195−D8
A. recurvatus NRRL 4902 T
A. multicolar CBS 133.54T
A. mulundensis CBS 140610T
A. pluriseminatus DTO 010−I8
A. pluriseminatus CBS 100523T
A. israelensis CBS 140627T
A. israelensis CBS 140628
A. unguis DTO 319−H6
A. unguis DTO 017−A6
A. unguis DTO 323−A2
A. unguis DTO 320−A5
A. unguis DTO 325−C2
A. unguis CBS 595.65
A. unguis NRRL 2393 T
A. croceus CBS 134396T
A. aurantiobrunneus CBS 465.65 T
A. fructus NRRL 239 T
0.04
100
89
86
100
100
82
100
90
100
75
99
72
100
100
100
100
100
100
100
100

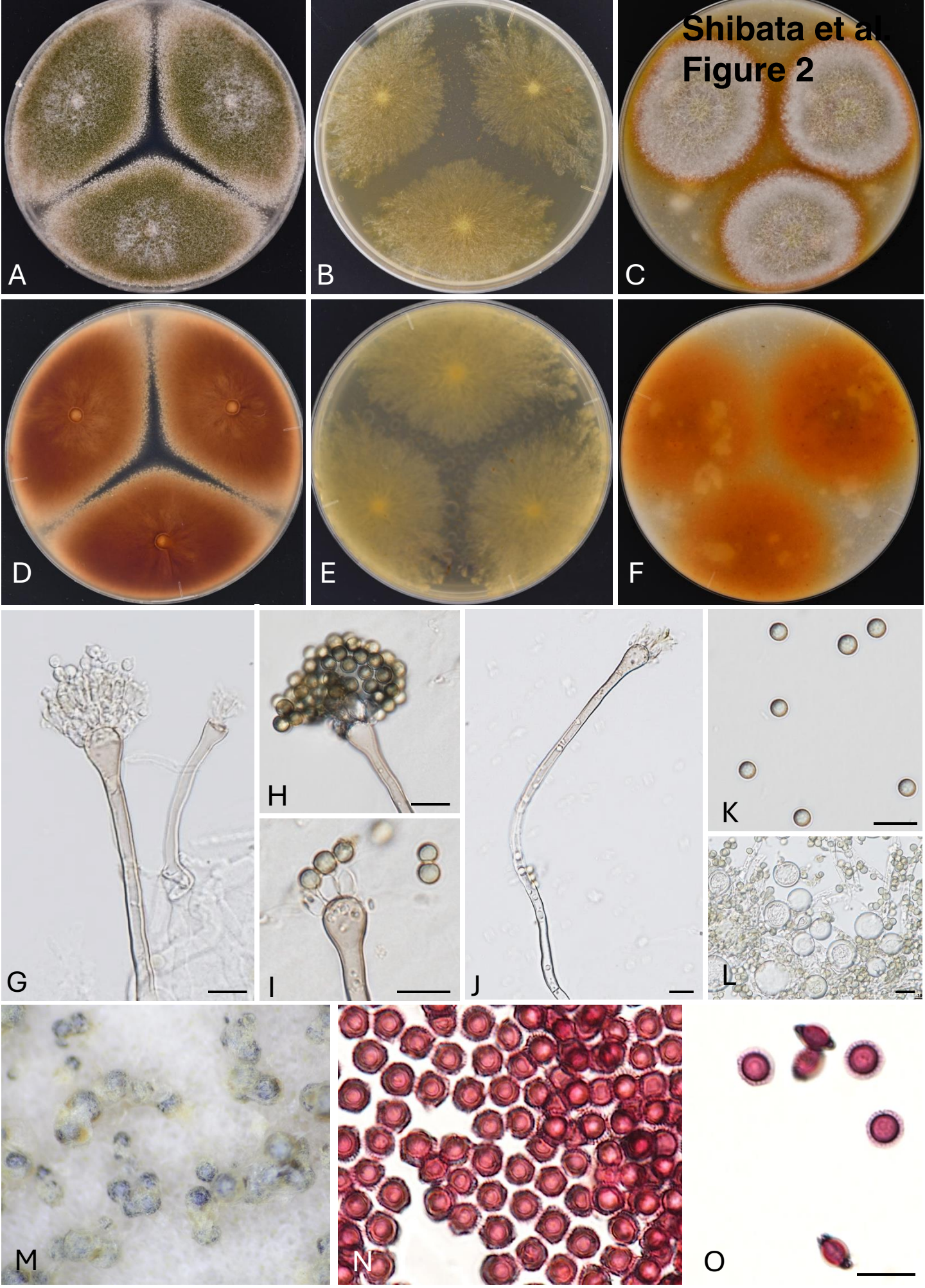
Shibata et al.
Figure 2
A
B
C
D
E
F
G
H
I
J
K
L
M
N
O